

# Crystal microstructure suitable for high-performance thermoelectric bulk materials

Osamu Yamashita · Hirotaka Odahara

Received: 22 July 2004 / Accepted: 18 April 2006 / Published online: 24 May 2007  
© Springer Science+Business Media, LLC 2007

**Abstract** The resultant thermoelectric power factor  $P$  and figure of merit  $Z$  of two types of composite device composed of a sandwich structure (A/B/A) were calculated by treating these devices electrical and thermal circuits. When the direction of the temperature gradient is perpendicular to a sandwiched slab with a lower  $\rho$  and a higher  $\kappa$  than those of the dominant material (a) and is parallel to a slab with a higher  $\rho$  and a lower  $\kappa$  than those of the dominant material (b),  $P$  increased significantly at an optimum slab thickness for device (a), in accordance with the result obtained by Bergman and Fel for a similar composite device, but decreased abruptly with increasing slab thickness for device (b), while  $Z$  remained almost unchanged with slab thickness for both devices as long as a thin slab is used. It was clarified that well-known high-performance thermoelectrics have crystal structures or microstructures corresponding to either device (a) or (b) fitted to enhance the boundary effect at the interface. Therefore, it is expected that when a number of thinly layered phases aligned in one direction are introduced into the microstructures of high-performance bulk materials; they enable the significant enhancement of boundary effect alone, resulting in a significant increase in  $Z$  of such bulk materials.

## Introduction

There has been considerable interest during the past 10 years in finding new materials and structures for use

in clear, highly efficient cooling and energy conversion systems [1]. The thermoelectric figure of merit  $ZT$  provides a measure of the quality of such materials for applications and is defined by  $ZT = \alpha^2 T / \rho \kappa$ , where  $\alpha$  is the Seebeck coefficient  $\rho$  is the electrical resistivity,  $\kappa$  is the thermal conductivity and  $T$  is the absolute temperature. Even a modest increase in  $ZT$  would be quite desirable for a number of applications previously. The  $n$ - and  $p$ -type materials with the highest  $ZT(=1)$  at room temperature were  $\text{Bi}_2(\text{Te}_{1-x}\text{Se}_x)_3$  and  $(\text{Bi}_{1-y}\text{Sb}_y)_2\text{Te}_3$  alloys [2]. However, we have most recently achieved significantly higher  $ZT$  of 1.19 at 298 K for  $n$ -type  $\text{Bi}_2(\text{Te}_{1-x}\text{Se}_x)_{33}$  [3] and 1.41 at 308 K for  $p$ -type  $(\text{Bi}_{1-y}\text{Sb}_y)_2\text{Te}_3$  [4], although it appears that these compounds may be approaching the limit of their potential performance.

Recently, the thermoelectric properties of quantum well and quantum wire superlattices have attracted considerable attention. There have been some theoretical predictions [5–9] that such superlattices will eventually have extremely high  $ZT$  as compared with those of the corresponding bulk materials due to the effects of the quantum confinement of carriers. Indeed, the significant increase in  $ZT$  has been observed in Si/Ge [10] and  $\text{Bi}_2\text{Te}_3/\text{Sb}_2\text{Te}_3$  [11] superlattice devices. However, these superlattice devices are very thin, being several micrometers at their thickest. For this reason, the application of these devices is limited to small cooling systems such as a pinpoint cooling system, since the heat capacity of a superlattice is too small to significantly cool various electronic devices with relatively large heat capacities, such as solid-state refrigerators. Therefore, the appearance of bulk thermoelectrics with high  $ZT$  is strongly desired because of their availability for any applications.

O. Yamashita (✉) · H. Odahara  
Faculty of Engineering, Ehime University, Bunkyocho,  
Matsuyama 790-8577, Japan  
e-mail: yamashio@eng.ehime-u.ac.jp

The use of a macroscopic composite device composed of a sandwich structure was considered as means of further increasing the  $Z$  of bulk thermoelectrics. The resultant  $Z$  and thermoelectric power factor  $P(=\alpha^2/\rho)$  for two types of device composed of slabs perpendicular and parallel to the direction of temperature gradient were calculated by treating their devices as electrical and thermal circuits. It was proved by such composite devices that well-known high-performance thermoelectrics have crystal structures or microstructures fitted extremely to enhance the boundary effect at their interface, resulting in an increase in  $Z$ .

The purpose of this paper is to show what microstructure is fitted to enhance the boundary effect at the interface, resulting in the further increase in the  $Z$  of bulk thermoelectrics through a significant decrease in the lattice thermal conductivity.

### Calculation of power factor and thermoelectric figure of merit

Sandwiched slab perpendicular to the direction of temperature gradient

Let us consider two-component composite thermoelectric devices (CTDs) composed of a sandwich structure (A/B/A) in which a slab of the material B is sandwiched between two parallelepipeds of the high-quality thermoelectric dominant material A, as shown in Fig. 1a. First, one calculates the macroscopic thermoelectric figure of merit for CTD (a) by treating it as an electrical and thermal circuit, in which the direction of the temperature gradient is perpendicular to a sandwiched slab. The thermoelectric materials A and B have the same cross-sectional area  $S$  and different thicknesses  $t_A$  and  $t_B$ , respectively. With  $\alpha$ ,  $\kappa$  and  $\rho$  of the two materials A and B given as  $\alpha_A$  and  $\alpha_B$ ,  $\kappa_A$  and  $\kappa_B$  and  $\rho_A$  and  $\rho_B$ , respectively, the total electrical resistivity  $\rho$  of CTD (a) is expressed as

$$\rho = \frac{2\rho_A t_A}{t} + \frac{\rho_B t_B}{t} \quad (1)$$

Here if we suppose  $2t_A = t(1-x)$  and  $t_B = tx$ , where  $t$  is the total thickness and  $x$  is the ratio of the  $t_B$  of a slab to the total thickness  $t$  and  $\alpha_B/\alpha_A = a$ ,  $\rho_B/\rho_A = b$  and  $\kappa_B/\kappa_A = c$ , Eq. (1) can be rewritten as

$$\rho = \rho_A \{(1-x) + bx\} \quad (2)$$

In the same manner, the total thermal conductivity  $\kappa$  is given by

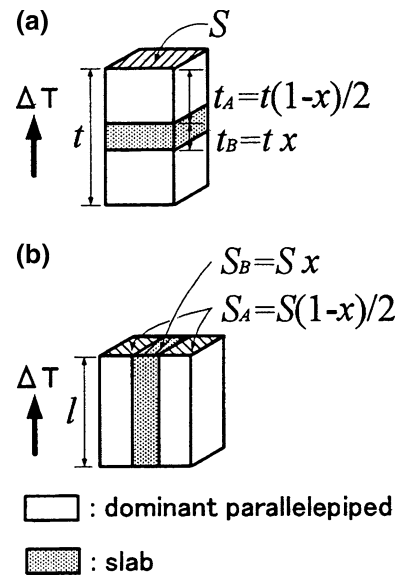


**Fig. 1** Composite thermoelectric device (CTD) of a sandwich structure (A/B/A) in which a slab of material B is sandwiched between two parallelepipeds of high-quality dominant material A. The slabs of CTDs (a) and (b) were sandwiched between two dominant materials perpendicular and parallel to the direction of the temperature gradient, respectively

$$\frac{1}{\kappa} = \frac{2t_A}{\kappa_A t} + \frac{t_B}{\kappa_B t} = \frac{1}{\kappa_A} \left\{ (1-x) + \frac{x}{c} \right\} \quad (3)$$

These equations are derived on the assumption that the scattering of carriers and phonons never occurs at the interface between a slab and two parallelepipeds. For a given temperature difference  $\Delta T$ , the temperature difference generated in each thermoelectric should be proportional to thickness but inversely proportional to thermal conductivity. Taking this into account, the ratio of  $\Delta T_A$  to  $\Delta T_B$  is expressed as

$$\frac{\Delta T_A}{\Delta T_B} = \frac{t_A \kappa_B}{t_B \kappa_A} \quad (4)$$

The total temperature difference  $\Delta T$  between both ends of CTD (a) is given by

$$\Delta T = 2\Delta T_A + \Delta T_B \quad (5)$$

The total thermal voltage  $\Delta V$  generated by  $\Delta T_A$  and  $\Delta T_B$  is expressed as

$$\Delta V = 2\Delta T_A \alpha_A + \Delta T_B \alpha_B \quad (6)$$

Therefore, the overall Seebeck coefficient  $\alpha$  is expressed as

$$\alpha = \frac{\Delta V}{\Delta T} = \frac{2t_A \kappa_1 B \alpha_A + t_B \kappa_A \alpha_B}{2t_A \kappa_B + t_B \kappa_A} = \alpha_A \frac{c(1-x) + ax}{c(1-x) + x} \tag{7}$$

using Eqs. (5) and (6). The thermoelectric power factor  $P$  and figure of merit  $Z$  are defined as  $P = \alpha^2/\rho$  and  $Z = \alpha^2/\rho \kappa$ , respectively. Substituting Eqs. (2), (3) and (7) into the equations of  $P = \alpha^2/\rho$  and  $Z = \alpha^2/\rho \kappa$ , the macroscopic resultants  $P$  and  $Z$  are expressed using the  $P_A$  and  $Z_A$  of the high-quality dominant material as

$$\frac{P}{P_A} = \left\{ \frac{c(1-x) + ax}{c(1-x) + x} \right\}^2 \frac{1}{\{(1-x) + bx\}} \tag{8}$$

and

$$\frac{Z}{Z_A} = \left\{ \frac{c(1-x) + ax}{c(1-x) + x} \right\}^2 \left\{ \frac{c(1-x) + x}{c(1-x) + bcx} \right\}, \tag{9}$$

respectively, where  $P_A = \alpha_A^2/\rho_A$  and  $Z_A = \alpha_A^2/\rho_A \kappa_A$ . Of course,  $P$  and  $Z$  are equal to  $P_A$  and  $Z_A$  at  $x = 0$ , and to  $P_B$  and  $Z_B$  at  $x = 1$ , where  $P_B = \alpha_B^2/\rho_B = a^2 P_A/b$  and  $Z_B = \alpha_B^2/\rho_B \kappa_B = a^2 Z_A/bc$ . It may be demonstrated by simple analyses that the conditions necessary for making  $P/P_A$  and  $Z/Z_A$  larger than 1 are  $a > 1 + c(b-1)/2$  and  $a > (1 + bc)/2$  for  $x \ll 1$ , respectively. This indicates that  $P/P_A$  can have a local maximum greater than its maximum among the different pure components for any values of  $a$  when  $a \geq 0$  and  $2 + c(b-1) < 0$ , while  $Z/Z_A$  increases only when  $Z_B > Z_A$ , holds, but it has no local maximum of  $Z/Z_A$ . The present composite device, thus, has a favorable effect on  $P/P_A$ , in accordance with the result of Bergman and Fel [12], while  $Z/Z_A$  can never exceed its maximum among the different pure components [13].

Sandwiched slab parallel to the direction of temperature gradient

In the same way, we calculate the resultants  $P/P_A$  and  $Z/Z_A$  for CTD (b) as shown in Fig. 1b. A and B have the same length  $l$  and different cross-sectional areas  $S_A$  and  $S_B$  respectively. The total electric resistivity  $\rho$  and thermal conductivity  $\kappa$  for CTD (b) are expressed as

$$\frac{1}{\rho} = \frac{2S_A}{\rho_A S} + \frac{S_B}{\rho_B S} = \frac{1}{\rho_A} \left\{ (1-x) + \frac{x}{b} \right\} \tag{10}$$

and

$$\kappa = \frac{2\kappa_A S_A}{S} + \frac{\kappa_B S_B}{S} = \kappa_A \{(1-x) + cx\}, \tag{11}$$

respectively, where  $2S_A = S(1-x)$ ,  $S_B = Sx$ ,  $b = \rho_B/\rho_A$  and  $c = \kappa_B/\kappa_A$  where  $S$  is the total cross-sectional area. The temperature difference  $\Delta T$  generated in CTD (b) should be the same for each constituent component. Therefore, the overall Seebeck coefficient  $\alpha$  is expressed as

$$\alpha = \frac{\Delta V}{\Delta T} = \frac{2\rho_B S_A \alpha_A + \rho_A S_B \alpha_B}{2\rho_B S_A + \rho_A S_B} = \alpha_A \frac{b(1-x) + ax}{b(1-x) + x}, \tag{12}$$

using Millman’s theorem, Where  $a = \alpha_B/\alpha_A$ . Substituting Eqs. (10)–(12) into the above well-defined equations, the resultants  $P$  and  $Z$  are expressed using  $P_A$  and  $Z_A$  of the high-quality dominant material as

$$\frac{P}{P_A} = \left\{ \frac{b(1-x) + ax}{b(1-x) + x} \right\}^2 \left\{ (1-x) + \frac{x}{b} \right\} \tag{13}$$

and

$$\frac{Z}{Z_A} = \left\{ \frac{b(1-x) + ax}{b(1-x) + x} \right\}^2 \left\{ \frac{b(1-x) + x}{b(1-x) + bcx} \right\}, \tag{14}$$

respectively. The condition necessary for making  $P/P_A$  larger than 1 is  $a > (1 + b)/2$  for CTD (b), unlike that for CTD (a) and this indicates that  $P/P_A$  increases only when  $P_B > P_A$  holds, but it has no local maximum, of  $P/P_A$ . However, the condition necessary for making  $Z/Z_A$  larger than 1 is quite the same as that for CTD (a), since Eqs. (9) and (14) transform into each other by replacing  $b$  with  $c$ . It was thus found that both  $P/P_A$  and  $Z/Z_A$  for CTD (b) increases only when B is superior in  $P$  and  $Z$  to A, but they do not have a local maximum.

### Results and discussion

Dependence of  $\rho/\rho_A, \kappa/\kappa_A, \alpha/\alpha_A, P/P_A$  and  $Z/Z_A$  on volume fraction  $x$

In order to investigate what effects the parameters  $b$  and  $c$  have on the resultant  $Z/Z_A$ ,  $Z/Z_A$  was calculated using Eq. (9) as a function of  $b$  and  $c$  for CTD (a) of  $a = 0$  and  $x = 0.05$  and the contour map of  $Z/Z_A$  was plotted in Fig. 2. It can be seen from the figure that

$Z/Z_A$  has a plateau when  $b < 1$  and  $c > 1$ , while in the range of  $b > 1$  and  $c < 1$ , it falls abruptly with increasing  $b$  and decreasing  $c$  and approaches zero at  $b \approx 10^3$  and  $c \approx 10^{-3}$ . For this reason, the same figure is also obtained for CTD (b) by replacing  $b$  with  $c$ . This suggests that  $\rho$  changes its role to  $\kappa$  according to the direction of the temperature gradient. Thus, in subsequent calculation, two sets of  $a = 0$ ,  $b = 0.10$  and  $c = 10$  and  $a = 0$ ,  $b = 10$  and  $c = 0.10$  which give  $Z/Z_A$  values of 0.99 and 0.43, respectively, at  $x = 0.05$  for CTD (a), were employed as parameters to clarify the effect of a sandwiched slab on  $P/P_A$  and  $Z/Z_A$ .

The resultants  $\rho/\rho_A$ ,  $\kappa/\kappa_A$ ,  $\alpha/\alpha_A$ ,  $P/P_A$  and  $Z/Z_A$  were calculated using Eqs. (2), (3) and (7)–(9) as functions of  $x$  for CTD (a) of  $a = 0$ ,  $b = 0.10$  and  $c = 10$ , as shown in Fig. 3. The parameters  $a$ ,  $b$  and  $c$  indicate that the sandwiched material B with  $\alpha_B = 0$  has a lower  $\rho$  and a higher  $\kappa$  than the high-quality dominant material A. As shown in Fig. 3a,  $\rho/\rho_A$  decreases linearly with increasing  $x$ , but  $\kappa/\kappa_A$  increases monotonically with increasing  $x$  and abruptly near  $x = 1$ .  $\alpha/\alpha_A$  decreases slowly with increasing  $x$  and falls abruptly near  $x = 1$ . As shown in Fig. 3b,  $P/P_A$  has a local maximum of  $P/P_A = 1.82$ , at  $x = 0.8$ , owing to a significant decrease in  $\rho$ , because the present parameters satisfy  $a > 1 + c(b-1)/2$  necessary for making  $P/P_A$  larger than 1. It is thus found that the macroscopic thermoelectric power for CTD (a) can be enhanced strongly, so that it is much greater than the largest value among the different pure components. This coincides qualitatively with the result calculated by Bergman and Fel [12] for a similar composite device using the classical contin-

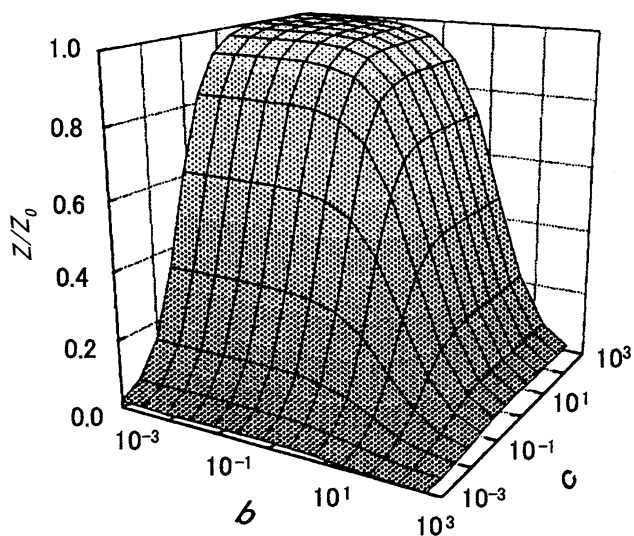


**Fig. 2** Contour map of  $Z/Z_A$  calculated as functions of  $b$  and  $c$  for CTD (a) of  $a = 0$  and  $x = 0.05$ . The same figure is also obtained for CTD (b) by replacing  $c$  with  $b$

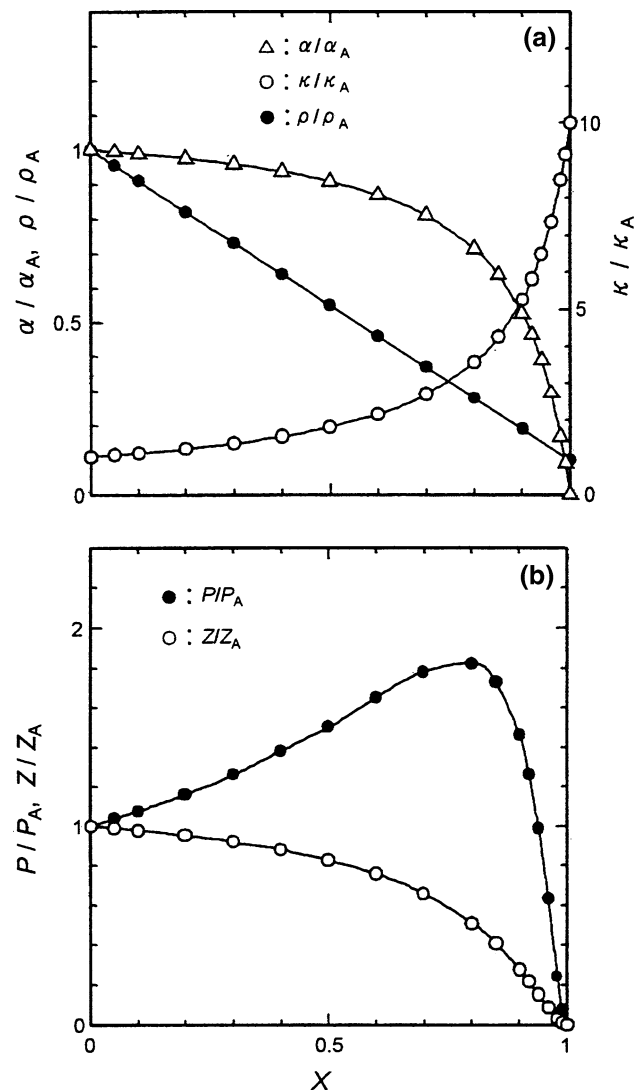


**Fig. 3** (a)  $\rho/\rho_A$ ,  $\kappa/\kappa_A$  and  $\alpha/\alpha_A$  and (b)  $P/P_A$  and  $Z/Z_A$  calculated as a function of  $x$  for CTD (a) of  $a = 0$ ,  $b = 0.10$  and  $c = 10$

uum linear transport theory. In contrast,  $Z/Z_A$  decreases slowly with increasing  $x$  and becomes zero at  $x = 1$ , so that  $Z/Z_A$  never exceeds 1, because the present parameters never satisfy  $a > (1 + bc)/2$  necessary for increasing  $Z/Z_A$ . However,  $Z/Z_A$  for CTD (a) changes little with  $x$  near  $x = 0$ . On the other hand, when  $a = 0$ ,  $b = 10$  and  $c = 0.10$  for CTD (a),  $\kappa/\kappa_A$  and  $\alpha/\alpha_A$  decrease abruptly with the increase in  $x$ , while  $\rho/\rho_A$  increases linearly with increasing  $x$ , so that the resultants  $P/P_A$  and  $Z/Z_A$  decrease abruptly near  $x = 0$ , as shown in Fig. 4.

Subsequently, the resultant thermoelectric properties were calculated for CTD (b) of  $a = 0$ ,  $b = 10$  and  $c = 0.10$ , where these parameters denote that a slab has a higher  $\rho$  and a lower  $\kappa$  than the dominant material. As shown in Fig. 5a,  $\kappa/\kappa_A$  decreases linearly with

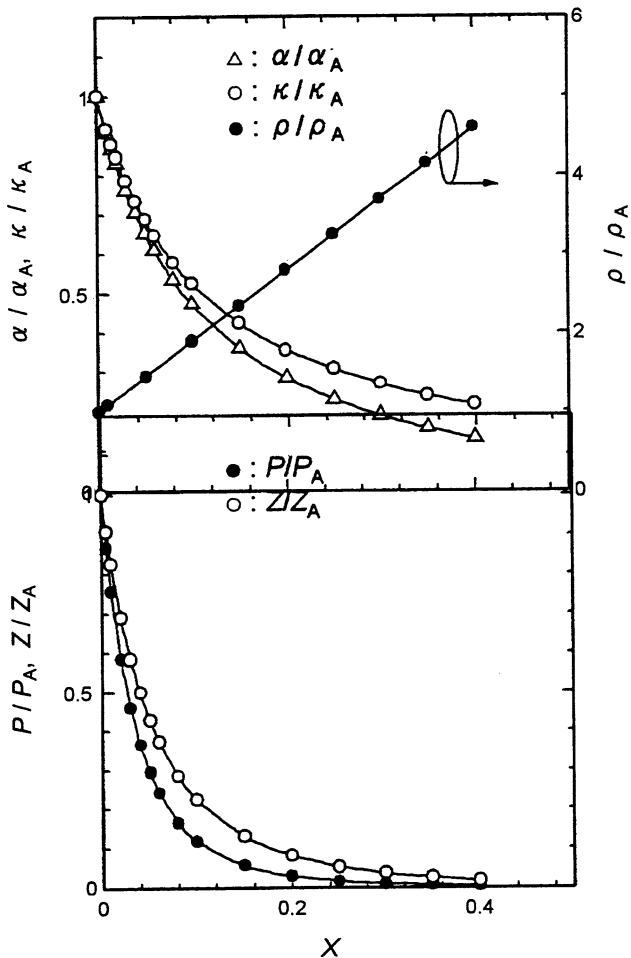


**Fig. 4** (a)  $\rho/\rho_A$ ,  $\kappa/\kappa_A$  and  $\alpha/\alpha_A$  and (b)  $P/P_A$  and  $Z/Z_A$  calculated as a function of  $x$  for CTD (a) of  $a = 0$ ,  $b = 10$  and  $c = 0.10$

increasing  $x$ , but  $\rho/\rho_A$  increases monotonically with increasing  $x$  and abruptly near  $x = 1$ .  $\kappa/\kappa_A$  and  $\rho/\rho_A$  in Fig. 5a for CTD (b) of  $a = 0$ ,  $b = 10$  and  $c = 0.10$  are replaced with  $\rho/\rho_A$  and  $\kappa/\kappa_A$  in Fig. 3a for CTD (a) of  $a = 0$ ,  $b = 0.10$  and  $c = 10$ , respectively. However, the  $x$ -dependence of  $\alpha/\alpha_A$  in Fig. 5a is quite the same as that shown in Fig. 3a. Therefore, the  $x$  dependence of  $Z/Z_A$  in Fig. 5b is the same as that of  $Z/Z_A$  in Fig. 3b. This is because the  $Z/Z_A$  calculated for CTD (a) of  $a = 0$ ,  $b = 0.10$  and  $c = 10$  is equivalent to that for CTD (b) of  $a = 0$ ,  $b = 10$  and  $c = 0.10$ . As shown in Fig. 5b, however,  $P/P_A$  decreases linearly with increasing  $x$  and has no local maximum, unlike that for CTD (a) of  $a = 0$ ,  $b = 0.10$  and  $c = 10$ . On the other hand, when  $a = 0$ ,  $b = 0.10$  and  $c = 10$  for CTD (b),  $\rho/\rho_A$  and  $\alpha/\alpha_A$  decrease monotonically with increasing  $x$ , while  $\kappa/\kappa_A$  increases linearly with increasing  $x$ , so that both  $P/P_A$  and  $Z/Z_A$  decrease abruptly near  $x = 0$ , as shown in Fig. 6, as in the case of CTD (a) of  $a = 0$ ,  $b = 10$  and  $c = 0.10$ .

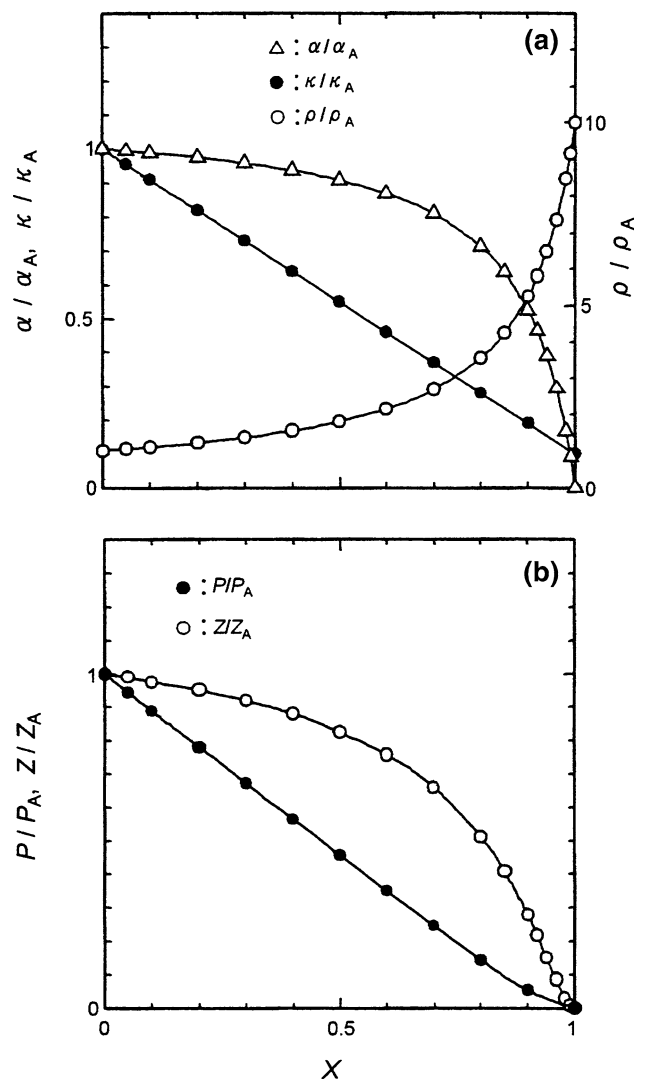


**Fig. 5** (a)  $\rho/\rho_A$ ,  $\kappa/\kappa_A$  and  $\alpha/\alpha_A$  and (b)  $P/P_A$  and  $Z/Z_A$  calculated as a function of  $x$  for CTD (b) of  $a = 0$ ,  $b = 10$  and  $c = 0.10$

Next, we discuss the composite effect of a sandwiched thermoelectric slab on  $P/P_A$  and  $Z/Z_A$  when a thin slab with a low  $\rho$  and a high  $\kappa$  was used for CTD (a) and a thin slab with a high  $\rho$  and a low  $\kappa$  was employed for CTD (b). The main role of a slab fitted to enhance the  $P$  of CTD (a) is to act as a low-thermal impedance series conduit for heat flow into the high quality thermoelectric dominant component, and also as a low-electrical impedance series conduit for the outflow of electric power. However, such a slab only slightly changes the overall  $S$  when it is thin even if the  $S$  of a slab is zero, because the temperature difference is very small in a thin slab. Owing to such thermoelectric properties of a slab,  $P/P_A$  for CTD (a) has a local maximum at a slab thickness while  $Z/Z_A$  remains almost unchanged with  $x$  near  $x = 0$ , at least

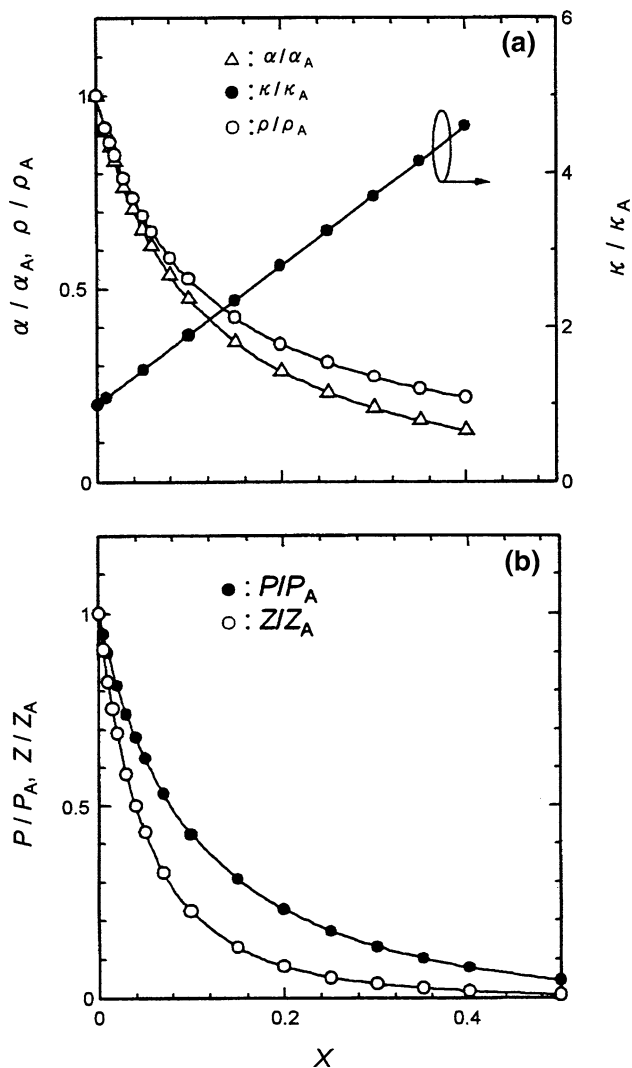


**Fig. 6** (a)  $\rho/\rho_A$ ,  $\kappa/\kappa_A$  and  $\alpha/\alpha_A$  and (b)  $P/P_A$  and  $Z/Z_A$  calculated as a function of  $x$  for CTD (b) of  $a = 0$ ,  $b = 0.10$  and  $c = 10$

for a thin slab. On the contrary, a slab having no adverse effect on the  $Z$  of CTD (b) acts as a high-thermal impedance row conduit for heat flow in the direction of the temperature gradient and also as a high-electrical impedance row conduit for electrical current. As a result,  $Z/Z_A$  for CTD (b) changes little with  $x$  at least for a thin slab, while  $P/P_A$  tends to decrease linearly with the increase in  $x$ .

In brief it was clarified here that the  $P/P_A$  and  $Z/Z_A$  of such composite devices depend strongly not only on the thermoelectric properties of a slab, but also on whether a sandwiched slab is parallel or perpendicular to the direction of the temperature gradient. The resultant  $Z$  unaffected by the introduction of a thin slab can enhance the boundary effect alone, not so as to degrade intrinsic  $Z$ . This is useful as a guide for determining the crystal microstructure that is most

desirable for increasing the  $P$  and  $Z$  of bulk thermoelectrics as high as possible.

#### Relation between composite device and crystal structures of high performance thermoelectrics

The boundary effect at the interface between the two materials A and B is not taken into account in the above calculation, but it should have a favorable effect on  $Z$  when thin composite microstructures were realized in thermoelectric crystals. It is shown here that the crystal structures and microstructures of well-known high-performance materials correspond to either microstructure (a) or (b), as shown schematically in Fig. 7.

When the superlattice material was fabricated by stacking a number of thin films, an increase in  $ZT$  along the stacked direction ( $c$ -axis) was observed by Venkatasubramanian et al. [11], who showed that the  $\rho$  of the superlattice material is about equal to that of the corresponding bulk material but its  $\kappa$  is much smaller than those of the constituent bulk materials, owing to the boundary effect, and the thin-film material composed of  $10/50 \text{ \AA}$   $\text{Bi}_2\text{Te}_3/\text{Sb}_2\text{Te}_3$  superlattices has an extraordinarily high  $ZT$  of 2.4 at room temperature. Indeed, the relative ratios of  $\text{Sb}_2\text{Te}_3$  to  $\text{Bi}_2\text{Te}_3$  for  $\rho$  and  $\kappa$  are 0.17 and 2.0, respectively [14]. Therefore, this microstructure is found to correspond to microstructure (a), as shown in Fig. 7.

Recently, oxide compounds such as  $\text{NaCo}_2\text{O}_4$  and  $\text{Ca}_2\text{Co}_2\text{O}_5$  with layered structures [14–17] have attracted attentions as promising thermoelectric materials because of their high potentials. The crystal structures of  $\text{NaCo}_2\text{O}_4$  and  $\text{Ca}_2\text{Co}_2\text{O}_5$  consist of

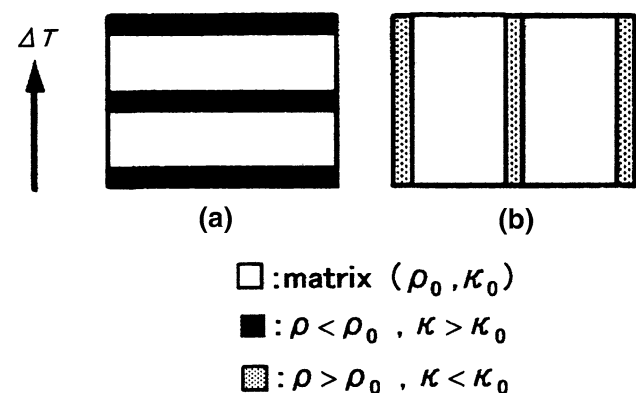


**Fig. 7** Two types of microstructure fitted to enhance the boundary effect; (a) thin layers perpendicular to the direction of the temperature gradient have a lower  $\rho$  and a higher  $\kappa$  than those of the matrix, and (b) thin layers parallel to the direction of the temperature gradient have a higher  $\rho$  and a lower  $\kappa$  than those of the matrix

two-dimensional  $\text{CoO}_2$  and Na ion layers and similar  $\text{CoO}_2$  and  $\text{Ca}_2\text{Co}_2\text{O}_2$  rocksalt layers, respectively, where their layers alternate in the  $c$ -axis direction. The two dimensional  $\text{CoO}_2$  layers act predominantly as an electrical conduction layer and the insulating Na ion and  $\text{Ca}_2\text{Co}_2\text{O}_2$  layers act to enhance the Seebeck coefficient [16]. Such a periodic two-layer structure is also effective in enhancing the phonon scattering at the boundary between their layers, leading to a lowering in  $\kappa$  along the  $ab$ -axis. Indeed, Na ion layers are surmised to have a low  $\kappa$  along the  $ab$ -axis from the fact that in the  $\text{Na}_x\text{CoO}_{2-\delta}$  single crystal the lattice  $\kappa_{\text{ph}}$  along the  $ab$ -axis is only one quarter of the electron  $\kappa_{\text{el}}$  along the  $ab$ -axis at 800 K [17]. Fujita et al. [17] reported that  $Z$  along the  $ab$ -axis of the  $\text{Na}_x\text{CoO}_{2-\delta}$  single crystal reaches a high value of  $1.5 \times 10^{-3} \text{ K}^{-1}$  at 800 K, corresponding to a surprisingly high value of  $ZT = 1.2$ . These insulating layers act as a slab of device (b), as shown in Fig. 1. Thus, the crystal structures of these oxides just correspond to microstructure (b), as shown in Fig. 7.

Next, it is shown that the same is true for the rhombohedral  $\text{Bi}_2\text{Te}_3$  crystal structure. The  $\text{Bi}_2\text{Te}_3$  crystal structure forms “quintuple-layer” leaves along the  $c$ -axis, where the layers in each leaf occur in the order  $\text{Te}^{\text{I}}\text{-Bi-Te}^{\text{II}}\text{-Bi-Te}^{\text{I}}$  [18]. The  $\text{Te}^{\text{II}}\text{-Bi}$  bond is covalent and the  $\text{Te}^{\text{I}}\text{-Bi}$  bond is mixed covalent and ionic; the bond between their leaves, i.e., the  $\text{Te}^{\text{I}}\text{-Te}^{\text{I}}$  bond is of the van der Waals type [18]. The thermoelectric high performance of  $\text{Bi}_2\text{Te}_3$  is a result of this weak van der Waals force, which is effective in enhancing the boundary effect at the interface between their leaves, leading to a significant lowering in  $\kappa$ . Such is the case.  $\kappa$  along the  $c$ -axis is less than one-half that along the  $ab$ -axis [19]. In contrast,  $\rho$  along the  $c$ -axis is much larger than twofold that along the  $ab$ -axis because of the presence of insulating  $\text{Te}^{\text{I}}\text{-Te}^{\text{I}}$  layers [19]. The  $\text{Te}^{\text{II}}\text{-Bi}$  layer forming a covalent bond, therefore, is considered to be responsible predominantly for electrical conduction along the  $ab$ -axis of the crystal. However, no significant anisotropy has been observed in Seebeck coefficient [19]. In practice, bismuth telluride exhibits a high  $Z$  along the  $ab$ -axis. The insulating  $\text{Te}^{\text{I}}\text{-Te}^{\text{I}}$  layers act as a slab of device (b) as shown in Fig. 1. Therefore, the crystal structure itself of  $\text{Bi}_2\text{Te}_3$  is considered to correspond to microstructure (b), as shown in Fig. 7, similarly to the layered oxides.

It is thus found that the microstructures and crystal structures of high-quality superlattices and bulk materials correspond to either microstructure (a) or (b) and are characterized by the layered structure fitted to enhance the boundary effect. As we shall see in the

following section, this provides a simple physical picture of the enhancement phenomenon in  $Z$ .

#### Crystal microstructure suitable for high-performance bulk thermoelectrics

There is a limit to the increase in the  $Z$  of high-quality bulk materials due to the improvement of the fabrication method. To exceed such a limit, it is necessary to further introduce the boundary effect into the microstructure, as thin layers consisting of precipitated phases or dopant segregations. For this reason, it is necessary to introduce a number of thinly layered phases aligned along almost the same direction into the bulk matrix. The growth condition or annealing condition of a thermoelectric ingot must therefore be controlled carefully, so that such phases are precipitated uniformly in either direction, that is, parallel or perpendicular to the freezing direction. Probably it is possible to find dopants or elements fitted to cause such precipitation. As mentioned earlier, the precipitated phases are required to have either a lower  $\rho$  and a higher  $\kappa$  or a higher  $\rho$  and a lower  $\kappa$  than those of the constituent matrix rather than to have a larger  $S$ . There are many types of material useful as precipitated phases; for examples, metallic materials are suitable for the former phase and ceramic compounds for the latter one. However, it is important whether such additives suitable for a high performance bulk material can be found.

The direction of the temperature gradient imposed on such thermoelectrics must be changed with the thermoelectric properties of the precipitated phases, as shown in Fig. 7. It is considered that for an optimum microstructure, the thickness of precipitated layers are smaller than the average carrier wavelength of  $\sim 100 \text{ \AA}$  estimated from the optimum carrier concentration of  $\sim 10^{25} \text{ m}^{-3}$  but are much longer than the phonon Debye wavelength of several angstroms. In such an ideal microstructure, carriers responsible for electrical conduction are slightly scattered at the interface but phonons are scattered predominantly. When such a composite microstructure was realized in bulk materials, therefore, the boundary effect at the interface should be enhanced significantly, resulting in a significant decrease in  $\kappa$ , as observed already in  $\text{BiTe-SbTe}$  superlattices [11]. However, even if the precipitated phases are considerably larger than the average carrier wavelength, they would not decrease  $Z$  as long as their volume fraction is very small, because the precipitated phases with optimum thermoelectric properties have little effect on intrinsic  $Z$  when the temperature gradient is imposed along an appropriate direction. It

may also be associated with such a phenomenon that we have succeeded in significantly increasing the  $Z$  of bismuth telluride compounds [3, 4], by producing thin dopant segregations throughout the crystal.

### Summary and conclusion

We have shown using a simple composite device that a significant increase in the resultant  $P$  can be achieved in a slab with a lower  $\rho$  and a higher  $\kappa$  than two dominant materials when a sandwiched slab is perpendicular to the direction of the temperature gradient. However, the resultant  $Z$  of composite devices can never exceed the largest value among those of two pure components for any components and arrangements. These results coincide qualitatively with previous results [12, 13]. In addition, it was shown that well-known high-performance thermoelectrics have crystal structures or microstructures corresponding to either device (a) or (b) as shown in Fig. 7. When the temperature gradient was imposed on a device along an appropriate direction according to the thermoelectric properties of a slab,  $Z$  remained almost unchanged with slab thickness as long as a thin slab is used. From these results, it is considered that when thinly layered phases with optimum thermoelectric properties are precipitated and aligned to one direction among various matrices, they should enhance readily and significantly the boundary effect alone, resulting in a significant increase in the  $Z$  of bulk thermoelectric materials. This is because thinly layered microstructures themselves hardly degrade intrinsic  $Z$ , as long as

they have a small volume fraction under the temperature gradient in the appropriate direction. If such thin microstructures were realized in high-performance bulk thermoelectric materials, it would be possible to achieve an extremely high  $ZT(>2)$  in bulk materials.

### References

1. Wood C (1988) Rep Prog Phys 51:459
2. Goldsmid HJ (1964) Thermoelectric refrigeration. Plenum, New York, p 15
3. Yamashita O, Tomiyoshi S (2003) Jpn J Appl Phys 42:492
4. Yamashita O, Tomiyoshi S, Makita K (2003) J Appl Phys 93:368
5. Hicks LD, Dresselhaus MS (1993) Phys Rev B 47:12727
6. Hicks LD, Harman TC, Dresselhaus MS (1993) Appl Phys Lett 63:3230
7. Hicks LD, Dresselhaus MS (1993) Phys Rev B 47:16631
8. Broido DA, Reinecke TL (1995) Appl Phys Lett 67:1170
9. Koga T, Rabin O, Dresselhaus MS (2000) Phys Rev B 62:16703
10. Koga T, Cronin SB, Dresselhaus MS, Liu JL, Wang KL (2000) Appl Phys Lett 77:1490
11. Venkatasubramanian R, Siivola E, Colpitts T, O'quinn B (2001) Nature 413:597
12. Bergman DJ, Fel LG (1999) J Appl Phys 85:8205
13. Bergman DJ, Leevy O (1991) J Appl Phys 70:6821
14. Ivanova LD, Granatkina YV (1995) Inorg Mater 31:678
15. Terasaki I, Sasago Y, Uchinikura K (1997) Phys Rev B 56:R12685
16. Funahashi R, Matsubara I (2001) Appl Phys Lett 79:362
17. Fujita K, Mochida T, Nakamura K (2001) Jpn J Appl Phys 40:4644
18. Wiese JR, Muldawer L (1960) J Phys Chem Solids 15:13
19. Ivanova LD, Granatkina YV, Sussmann H, Muller E (1993) Inorg Mater 29:969